Heliyon 6 (2020) e04329

Contents lists available at ScienceDirect

Heliyon

journal homepage: www.cell.com/heliyon

Research article

Topography-driven alterations in endothelial cell phenotype and contact guidance

Ana Maria Almonacid Suarez [a], Iris van der Ham [a], Marja G.L. Brinker [a], Patrick van Rijn [b,*], Martin C. Harmsen [a,**]

[a] University of Groningen, University Medical Center Groningen, Department of Pathology and Medical Biology, Hanzeplein 1 (EA11), 9713 GZ, Groningen, the Netherlands

[b] University of Groningen, University Medical Center Groningen, Department of Biomedical Engineering-FB40, W.J. Kolff Institute for Biomedical Engineering and Materials Science-FB41, A. Deusinglaan 1, 9713 AV, Groningen, the Netherlands

ARTICLE INFO

Keywords:
Bioengineering
Biophysics
Cell biology
Biomedical engineering
Regenerative medicine
Directional topography
Endothelial cells
Vascular-like networks
Contact guidance
Vascularization

ABSTRACT

Understanding how endothelial cell phenotype is affected by topography could improve the design of new tools for tissue engineering as many tissue engineering approaches make use of topography-mediated cell stimulation. Therefore, we cultured human pulmonary microvascular endothelial cells (ECs) on a directional topographical gradient to screen the EC vascular-like network formation and alignment response to nano to microsized topographies. The cell response was evaluated by microscopy. We found that ECs formed unstable vascular-like networks that aggregated in the smaller topographies and flat parts whereas ECs themselves aligned on the larger topographies. Subsequently, we designed a mixed topography where we could explore the network formation and proliferative properties of these ECs by live imaging for three days. Vascular-like network formation continued to be unstable on the topography and were only produced on the flat areas and a fibronectin coating did not improve the network stability. However, an instructive adipose tissue-derived stromal cell (ASC) coating provided the correct environment to sustain the vascular-like networks, which were still affected by the topography underneath. It was concluded that large microsized topographies inhibit vascular endothelial network formation but not proliferation and flat and nano/microsized topographies allow formation of early networks that can be stabilized by using an ASC instructive layer.

1. Introduction

Vascularization of tissue engineered constructs is crucial to enable the exchange of gases and nutrients needed for large tissue survival *in situ* and to allow for proper integration into the body [1]. Studying the endothelial cell response to nano- and microtopographies may facilitate the development of strongly vascularized replacement tissues such as myocardial or skeletal stents to treat the consequences of myocardial infarction or muscle damage [2]. In particular, in muscle tissue, capillaries comprised of endothelial cells (ECs) align to the linear and parallel muscle fibers, which is essential to maintain a healthy phenotype [3]. The extracellular microenvironment of the blood vessel is comprised of spatially well-organized collagen bundles that vary in size and are therefore classified according to their microstructure: intima (disperse fibers), media (fiber bundles at 30°), and adventitia (axially aligned fibers) layers [4]. Microvasculature, i.e. arterioles, capillaries, and venules are the work horses of tissue perfusion and primarily consist of endothelial cells with a low fraction of pericytes that maintain endothelial function. The microvasculature endothelial cells are bound to a basement membrane at their basal side. Therefore, control of the organization of microvasculature is key for the upscaling of tissue engineered constructs.

Endothelial cells migrate from pre-existing vessels once activated by exogenous triggers such as VEGF-A and Ang-2 [5], and proliferate to form new branches via polarized tip cells and stalk cells in a process called angiogenesis [6]. The migration of ECs is fundamental for angiogenesis and is regulated by chemotactic, hapotactic, and durotactic stimuli [5]. Another later discovered process, topotaxis [7], corresponds to cell orientation and cytoskeleton polarity and causes cell migration, including ECs, due to topographic cues [8]. Topography has been

* Corresponding author.
** Corresponding author.
E-mail addresses: p.van.rijn@umcg.nl (P. van Rijn), m.c.harmsen@umcg.nl (M.C. Harmsen).

https://doi.org/10.1016/j.heliyon.2020.e04329
Received 9 June 2020; Received in revised form 18 June 2020; Accepted 24 June 2020

investigated before for the migration of ECs but with a limited number of topography dimensions, which therefore does not provide a broad view [9, 10, 11, 12].

Literature shows a large variety of ranges and architectures affecting the EC alignment. ECs have been aligned by using: nanofibrils made of 30–50 nm collagen I fibers [13]; micropatterns mostly made of fibronectin with 2.5 μm–100 μm stripes [14, 15, 16]; microgrooves with ridges and grooves ranging from 200 nm to 10 μm and depths of 50 nm to 5 μm [17, 18, 19, 20, 21]; and fewer topographies with sinusoidal features with 20 μm wavelength and 6.6 μm amplitude [22]. Previously, we have shown that directional gradients can be used for screening the morphological and phenotypical response of osteoblasts [23, 24], adipose tissue-derived stromal cells (ASCs) [25], and myoblasts [26]. Cell phenotype is significantly affected by topography, which has differing effects depending on the cell type. However, topography-driven responses of ECs remain but poorly investigated. As indicated, previous studies addressed topography-mediated behavior but with a limited number of topography sizes. The strength of using the topography gradient is that behavior of ECs can be monitored across a large range of feature sizes in one experiment rather than a few isolated arbitrarily chosen features. Particularly vital is the aspect of creating vascularized tissues of which the parenchymal cell is directed by topography and it is unclear how endothelial cells respond directly to topography or parenchymal cells supporting the formation of vascular-like networks while being in contact with topography. Hence, understanding which topographies induce specific behavior in endothelial cells is of great importance.

Finding the proper topography that allows endothelial cells to form tubular interconnected networks of tissue engineered skeletal muscle has been of interest to us and others, and it is a key component of tissue engineering. Therefore, we hypothesized that alignment and vascular-like network formation behavior of human microvascular endothelial cells is affected by directional topography features and the specific size of these topographical features. By using a directional topographical gradient, we could screen and assess different topographies to later design a mixed topography. The mixed topography induced two different EC behaviors in a single material substrate to elucidate the delicate interplay between these two topography stimuli and where we could explore the vascular-like network formation and proliferative properties of these ECs.

2. Results

2.1. Endothelial cell alignment and vascular-like network formation is localized on different areas on the directional topographical gradient

We used a directional topography gradient, as produced and used previously [26], to identify the influence of specific topography dimensions on endothelial cell vascular-like network formation. Previously, results showed that ECs do not attach to bare Polydimethylsiloxane (PDMS) (not shown). Thus, ECs were cultured on the directional topography gradients with different coating approaches to enhance attachment. ECs were cultured on coated PDMS substrates using gelatin (1 μg per ml) or using different concentrations of human fibronectin (1 μg per ml, 10 μg per ml, or 20 μg per ml).

At 48 h post-seeding, on the smaller topographies (nanosized) (wavelength 1.5 μm and amplitude 176 nm), irrespective of the coating, ECs did not align but randomly oriented. In fact, at 48 h ECs had aggregated and started to form tubular networks resembling an early stage of vascular-like network formation of ECs on substrates such as Matrigel (Figure 1a, left column). The only noticeable difference among the different coatings was that gelatin coatings were the first to induce aggregate formation (Figure 1a bottom row, left column) compared to fibronectin coated topographies. While the gelatin and fibronectin coating did not affect the behavior of ECs on flat (supplementary information Figure 2) nor directional topography, we continued with gelatin coatings. ECs had aligned to the larger (micronsized) directional topography of the gradient (wavelength 9.9 μm and amplitude 2.1 μm) (Figure 1a right column). Cells in the middle of the gradient, with intermediate sized topographies (ranging between wavelengths of 2.3 μm–3.8 μm and amplitudes of 400 nm–800 nm) showed both alignment and vascular-like networks. Apical protrusions, typical for stalk cells during angiogenic vascular-like network formation were clearly visible (Figure 1b, boxed insets). However, these vascular-like networks were not stable and collapsed after approximately one hour. The collapse of these networks resulted in cell aggregates that remained attached to the substrate.

At 96 h post-seeding, the density of ECs had increased and thereby repopulated the whole gradient surface, suggesting these cells had proliferated on the large directional topography. In addition, there was aggregate formation which suggests cell migration. Once in confluency, ECs again formed the vascular-like networks on the small (nanosized) to middle sized features (wavelengths ranging from 1.5 μm to 3.8 μm and amplitudes ranging from 176 nm to 780 nm, which correspond to positions 0–7 mm in the gradient, Table 1). This result indicates that the vascular-like network formation, followed by aggregation, is a cyclic phenomenon dependent on topography and cell confluency.

The vascular-like networks were observed on the directional topography gradients from small (nano-size) to middle size features irrespective of the coating (size corresponds to positions 0–7 mm in the gradient, Table 1) (Figure 2a). On the other hand, on the larger features of the directional topography gradient, cells remained aligned along the topography direction (wavelengths ranging from 4.8 μm to 9.9 μm and amplitudes ranging from 1015 nm to 2169 nm, which corresponds to positions 8–10 mm in the gradient, Table 1) (Figure 2a).

On flat PDMS controls, ECs had adhered and arranged in a randomly organized fashion, while these formed vascular-like network structures at 48 h- and 96 h post-seeding. These were similar to the vascular-like networks on the topographical gradients and collapsed soon after their formation as described earlier. The ECs on the flat PDMS (control) had the same behavior as in the directional topography gradients from small (nanosized) to middle sized directional topography features (0–7 mm of the gradient) by showing vascular-like networks (Figure 2b) and later cell aggregation. These cell aggregates remain attached at the surface of the directional topography and the flat PDMS over time (Supplementary information Figure 1). In contrast, ECs seeded on Tissue Culture Polystyrene (TCP) controls were arranged randomly and proliferated normally as during propagation for these experiments. On TCP, ECs did not spontaneously aggregate nor formed networks at any time (Figure 2c).

Our results show that on flat and nanometer-sized topographies, ECs spontaneously formed initial networks, although these networks were unstable (schematic overview provided in Figure 2d). As it appears, large, microsized, topographies inhibited vascular-like network formation but not proliferation. Well before reaching confluency, ECs started to form vascular-like networks that readily collapsed on the surface of ranging from the small to middle sized directional topography features (0–7 mm of the gradient). However, over time, 24–48 h, once confluent again, the unstable vascular-like networks were observed (Figure 2d). The ECs from these disintegrated unstable networks formed aggregates which remained attached to the substrate surface (Figure 2d). This unexpected behaviour indicates that topography variations may elicit highly different cell response when addressing topography-mediated tissue engineering approaches in which vascularization approaches are desired to be included.

2.2. Formation of mixed topography to proliferate and differentiate ECs

The observation that the biological response of ECs to different topographies varies between vascular-like network formation and proliferation was further assessed by seeding ECs onto a combination of flat and micron-sized topographies. These topographies were generated either parallel or perpendicularly to the flat PDMS. We anticipated that on the topographies, ECs would proliferate, while these would migrate to the flat surface and form vascular-like networks.

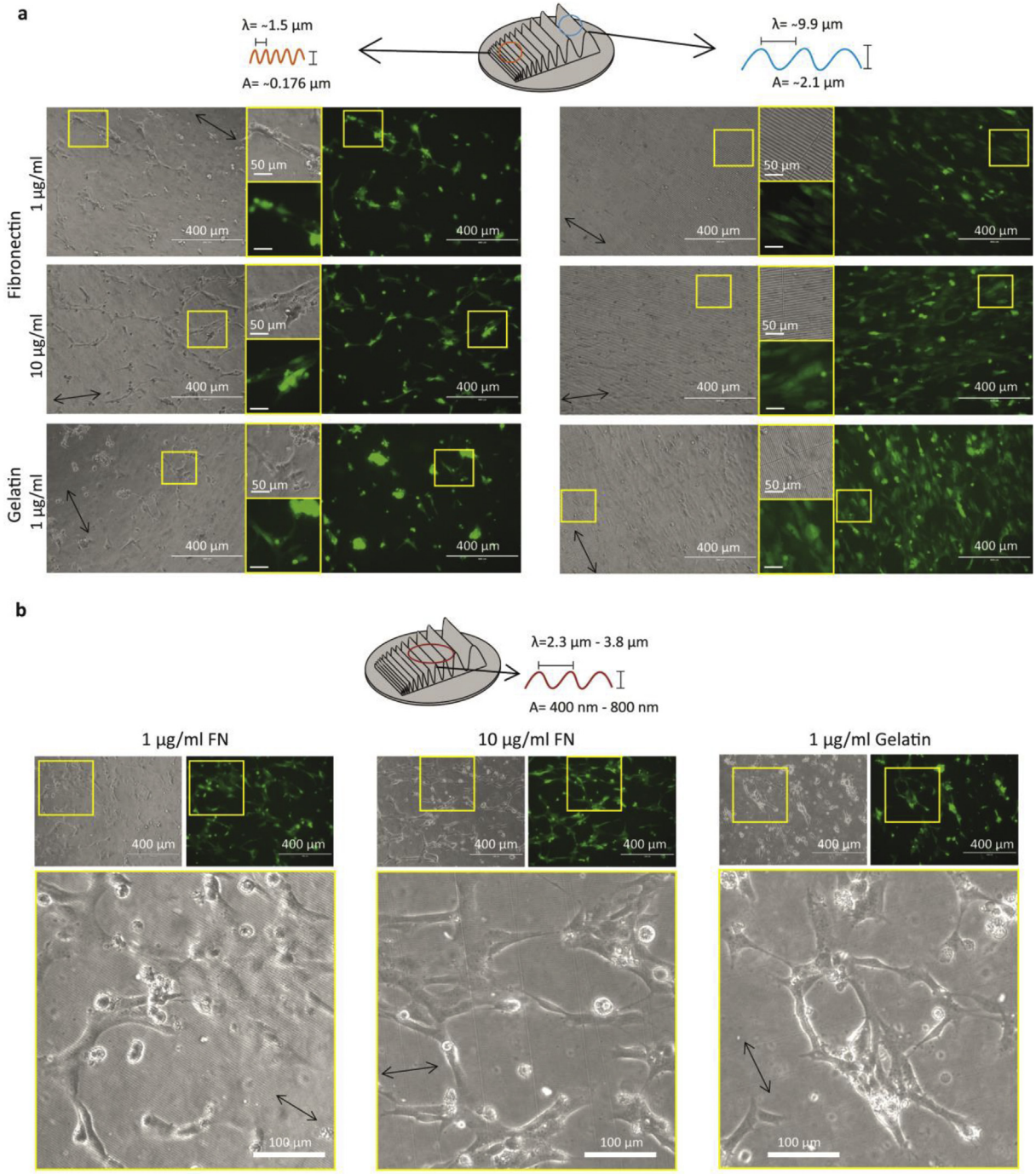

Figure 1. Bright field and fluorescence micrographs of ECs on the gradients after 48 h in culture. **a.** Left column corresponds to micrographs of ECs cultured on the smallest features of the directional topographical gradient (wavelength 1.5 μm and amplitude 176 nm) and the right column corresponds to micrographs of ECs cultured on the largest features of the directional topography gradient (wavelength 9.9 μm and amplitude 2.1 μm) with various coatings: (top) 1 μg per ml fibronectin, (middle) 10 μg per ml fibronectin, and (bottom) 1 μg per ml gelatin. Left images in the rows of each column correspond to bright-field images and the right-side images show the Enhanced Green Fluorescent Protein (EGFP) lentiviral transduced ECs. Scale bars are 400 μm. In the middle, zoomed-in images of the micrographs. Scale bars are 50 μm. **b.** Bright-field micrographs ECs culture on the middle part of the gradient (wavelengths of 2.3 μm–3.8 μm and amplitudes of 400 nm–800 nm). Top images show formation of vascular-like network structures. Scale bars are 100 μm. Bottom images show the zoom-in of stalk cells or tip cells located on the early vascular-like network formation. Scale bars are 50 μm.

The directional topography parallel to the flat had an average wavelength of 10.4 ± 0.2 μm and amplitude of 3.4 ± 0.1 μm (Figure 3a), and the directional topography perpendicular to flat had an average wavelength of 9.8 ± 1.3 μm and amplitude of 3.2 ± 0.3 μm (Figure 3b). The interface between the directional topography and the flat area had a sharp transition (Figure 3a). The microtopography dimensions reflect the area within the topography gradient where vascular-like network formation was absent and ECs were prone to follow the topography.

2.3. ECs display dynamic behavior on mixed topography surfaces

The nanotopography structures induced comparable behavior in ECs as on the flat controls while the micrometer topography had a different influence on EC behavior. While the flat stimulates aggregate formation, the microtopography supported better proliferation and cell alignment. Investigating the behavior of ECs on mixed topography namely flat and microtopography serves two purposes. First, the difference in behavior

towards both surfaces can be identified in the same experiment and second, it provides insights in dynamic behavior when cells encounter different topography input sequentially. ECs on gelatin-coated mixed topographies and flat PDMS, were recorded by live-imaging using a Solamere microscope over a period of 72 h. ECs on the mixed directional topography running both parallel and perpendicular to the flat, in the time evaluated, attached and aligned following the directionality of the topography. The flat area of the mixed surface showed the beginning of vascular-like network formation, yet complete networks were never formed. Instead, ECs formed aggregates that increased in size over a 24-hour period (Figure 4a, b).

During the 72 h evaluation, the aggregates moved around the mixed surfaces and once encountering the directional topography, they disintegrated into cells following the topography rather than remaining inside the cluster and attached and aligned to the directional topography (Figure 4 a and b, Supplementary information Videos 1–4). On the other hand, after approximately 14 h, ECs on the flat PDMS surfaces showed stalk and tip cell morphologies (Figure 4c) and vascular-like networks were formed. However, after approximately 22 h some of the networks collapsed and formed aggregates. Over time, the number of aggregates showed a tendency to decrease in number in the mixed topographies (Figure 4 d and e). No significant differences were found in the number of aggregates and surface area of the aggregates between the mixed directional topographies running either parallel or perpendicular to the flat area.

Supplementary content related to this article has been published online at https://doi.org/10.1016/j.heliyon.2020.e04329.

On other occasions, cells did not spread onto the surface and did not form vascular-like networks but directly aggregated (Supplementary information Video 5, bottom left corner). In addition, it was observed that aggregates can fuse (Figure 5. Supplementary video 6).

Supplementary content related to this article has been published online at https://doi.org/10.1016/j.heliyon.2020.e04329.

Comparing the aggregate formation between the different mixed topographies and the flat substrate could give insights into the response of ECs to the different topographies. It was observed that the number of aggregates was higher on the flat control surfaces with a mean number of aggregates 21.2 ± 3.2 on an area of 2.8 mm^2 compared with the mixed surfaces (substrate with both directional topography and flat) over a period of 40 h. On the micron-sized topography running parallel to the flat, the mean number of aggregates was 11.2 ± 1.2 over an area of 2.8 mm^2 and on the microsized topography perpendicular to the flat, the mean number of aggregates was 13.7 ± 3.0 over an area of 2.8 mm^2 (One-way ANOVA $p = 0.0083$. Tukey comparison test perpendicular $p = 0.0294$, parallel $p = 0.0082$) (Figure 4d). Additionally, the surface area of the aggregates was significantly larger on the flat control with an average of $1.07 \times 10^5 \pm 0.25 \times 10^5$ μm^2 (One-way-ANOVA $p = 0.0194$) compared to the substrates with mixed topography running parallel to the flat which had a mean aggregate surface area of $4.91 \times 10^4 \pm 0.27 \times 10^4$ μm^2 (Tukey comparison test parallel $p = 0.0160$) (Figure 4e).

2.4. Adhesion coating affects the dynamic behavior of ECs on mixed topography surfaces

We were able to establish that the aggregates were formed after 6 h of cell culture and that the aggregates separated into single cells once in contact with the directional topography. Cell aggregates increased in size by merging with other cell aggregates. However, with the mixed topographies, we were not yet able to control the vascular-like networks nor the aggregate formation. Therefore, the coating was altered with the aim of stabilizing the vascular-like networks. ECs were cultured on the mixed topography running perpendicular to the flat, coated with 20 μg per ml of human fibronectin instead of gelatin, and recorded over a period of three days.

Endothelial cells had an aligned orientation following the directionality of the topography and were randomly oriented on the flat part of the same substrate after 2 h and 30 min of cell culture (Figure 6a, Supplementary information video 7). The cells had spread well on the mixed topography for the first 15 h of cell culture, which was similar to TCP controls with both coatings, gelatin and fibronectin. At about 21 h post-

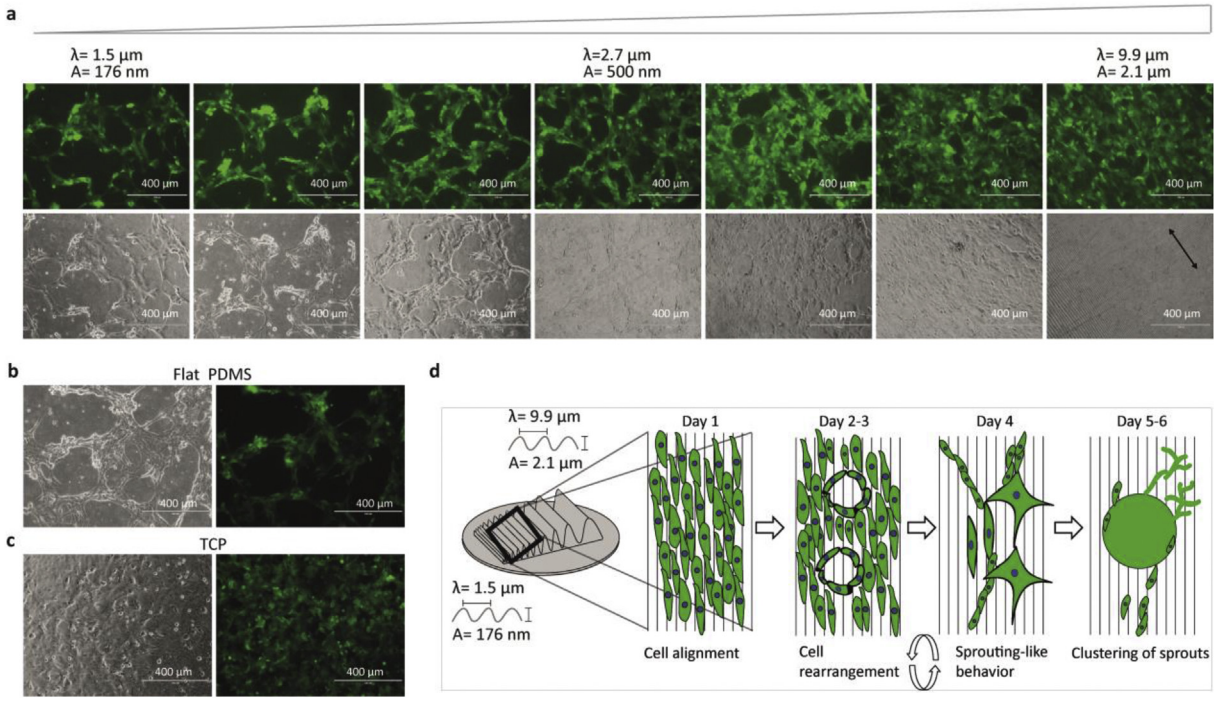

Figure 2. Micrographs of ECs on gradients with 1 μg per ml gelatin coatings. **a.** Micrographs correspond to images of the gradient with 1 μg per ml of gelatin coating after four days of culture. The triangle depicts wrinkle size development going from nanosized to microsized feautures. The top image corresponds to GFP image and bottom to bright field. **b.** PDMS flat control with 1 μg per ml of gelatin coating. **c.** TCP control with 1 μg per ml of gelatin coating. **d.** Schematic representation of the ECs' behavior on the directional topography gradient in the nanosized part and the middle of the gradient with micron-sized topography. Scale bars are 400 μm.

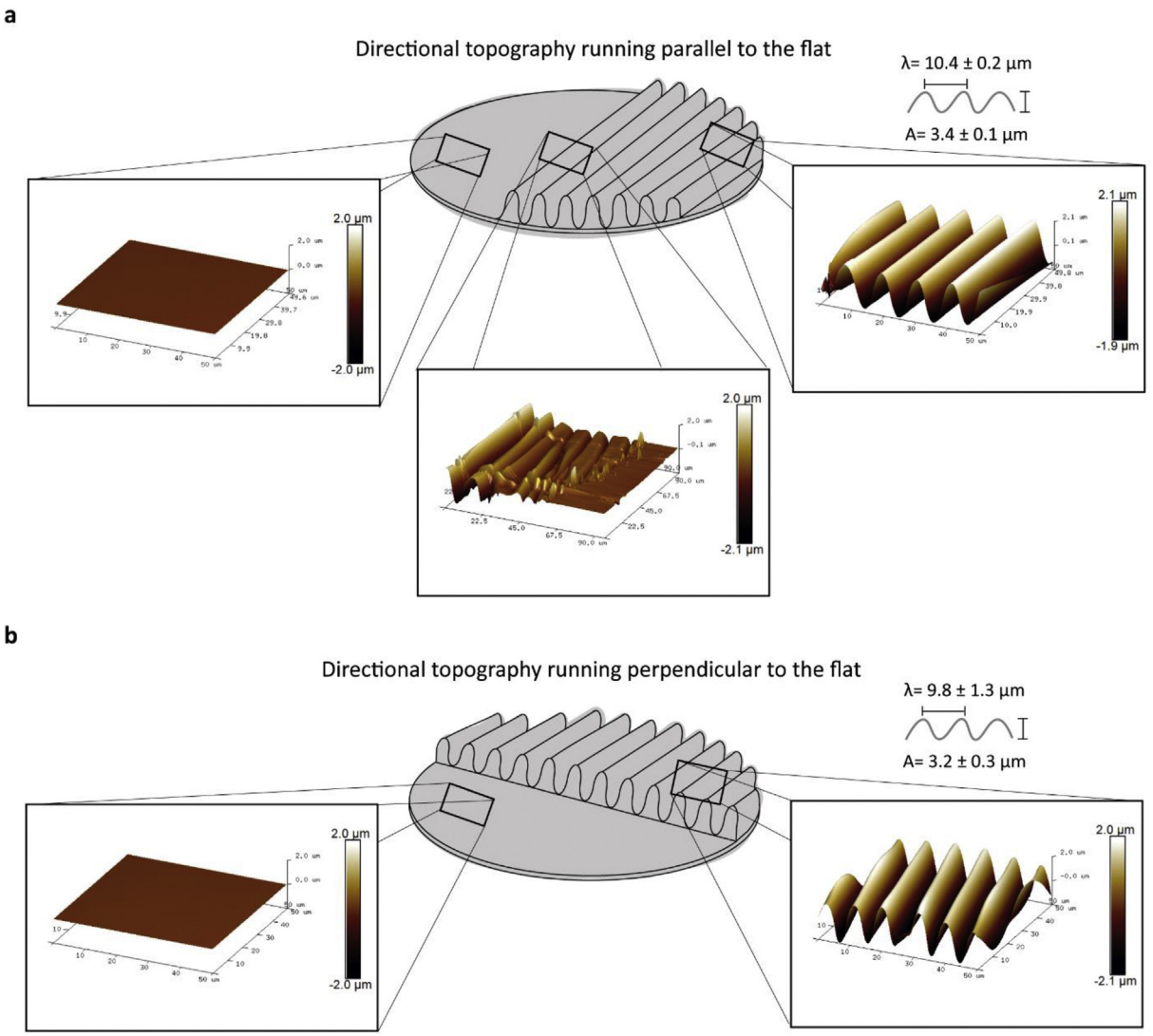

Figure 3. Atomic force microscopy of the mixed directional topography surfaces. **a.** Directional topography running parallel to the flat. AFM of the flat part, the interface between wrinkles and the flat surface, and the directional topography. **b**. Directional topography running perpendicular to the flat. AFM of the flat part of the surface, and the directional topography wrinkle sizes.

seeding, the continuous monolayer that had covered the boundaries between flat and topography started to show some networks formation that rapidly collapsed followed by detachment of the rest of the cellular monolayer from the flat part (Figure 6a, Supplementary information video 7). Subsequently, the cell layer on the flat area started to contract in the direction opposing the directional topography, thereby forming an aggregate.

Supplementary content related to this article has been published online at https://doi.org/10.1016/j.heliyon.2020.e04329.

On the other hand, the flat PDMS control showed small aggregate formation after around 2 h of cell culture even though half of the surface still contained well-spread ECs on its surface (Figure 6b). Instead of forming only aggregates, ECs detached as an intact monolayer, slowly forming an elongated aggregate structure (Supplementary information Video 8) as shown also on the flat area of the mixed substrate. After roughly 21 h, the aggregates hardly changed anymore (Supplementary information Figure 2).

Supplementary content related to this article has been published online at https://doi.org/10.1016/j.heliyon.2020.e04329.

Endothelial cells on the fibronectin coating attached and spread for the first hours in a similar fashion as those on the gelatin coating. However, the main difference between the two coatings, gelatin and fibronectin, was the aggregation behavior of the cells. Gelatin allowed the formation of several aggregates in spite of whether ECs spread and attached onto the flat surface properly or not. The fibronectin coating allowed ECs to spread and attach for a longer period (Supplementary information Figure 2 and Supplementary information video 9). It was anticipated that the lifetime of newly formed networks might depend on the coating concentration, which was not observed during the experiments. Adjusting the coating to 20 μg per ml fibronectin with respect to the previously used 10 μg per ml, had no effect on the stabilization of the networks formation and avoidance of aggregate formation. Therefore, higher fibronectin concentrations are not needed.

Supplementary content related to this article has been published online at https://doi.org/10.1016/j.heliyon.2020.e04329.

2.5. Dynamic behavior of ECs is altered on confluent (aligned) ASC monolayers

The formation of vascular-like networks by ECs on topographies requires a coating with gelatin, while fibronectin did not induce stable networks. Our earlier research showed that ECs form networks on monolayers of ASCs [27]. Therefore, we questioned if the influence of ASC monolayers would stabilize endothelial networks in the system

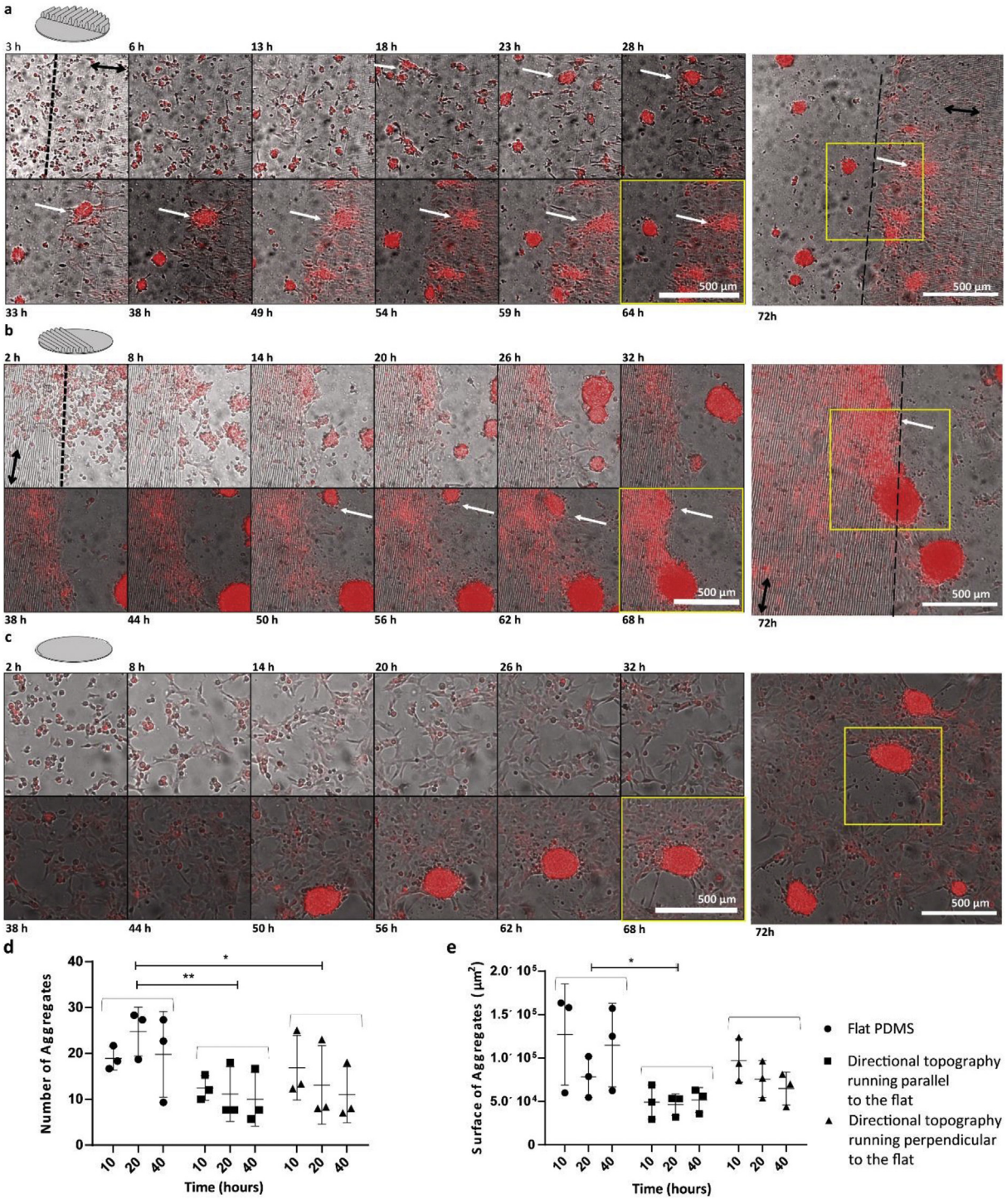

Figure 4. Directional mixed topography parallel and perpendicular to flat over 72 h of EC culture. **a.** ECs dTomato + on mixed directional topography perpendicular to the flat. Dotted line shows the interface between the directional topography and the flat area. Black arrow shows the directionality of the directional topography. White arrow shows an aggregate that has reached the topography and is in train to disintegrate. **b.** ECs dTomato + on mixed directional topography parallel to the flat. Dotted line shows the interface between the directional topography and the flat area. Black arrow shows the directionality of the directional topography **c.** ECs dTomato + on PDMS flat control. Culture hours are depicted on top and bottom of the micrographs. Montage of micrographs were resulted from the videos and a zoom-in area as depicted on the image after 72 h of cell culture. Scale bars are 500 µm. **d.** Number of aggregates quantified on the three different surfaces, flat PDMS, mixed directional topography parallel and perpendicular to the flat area on top of the flat parts, after 10, 20 and 40 h of cell culture. The number of aggregates was obtained from three independent experiments, each number is provided as a separate data point as well as the average (line) and it depicts the number of aggregates visible at the specific time-point as indicated. Significantly higher number of aggregates on the flat surface (One-way ANOVA $p = 0.0083$) in comparison with the mixed surfaces (Tukey comparison test perpendicular $p = 0.0294$, parallel $p = 0.0082$), combined populations at different time points were taken and flat compared to parallel and perpendicular. **e.** Surface area of aggregates on the three different surfaces, flat PDMS, mixed directional topography parallel and perpendicular to the flat area, after 10, 20 and 40 h of cell culture. Surface area was significantly larger on the flat surface (One-way-ANOVA $p = 0.0194$) in comparison with the mixed directional topography parallel to flat (Tukey comparison test parallel $p = 0.0160$), combined populations at different time points were taken and flat compared to parallel and perpendicular.

presented here and also enhance the seemingly inhibited vascular-like network formation induced by the microtopography. ASCs were seeded on the microsized directional topography (and flat controls) showed to have a significant influence on vascular-like network formation of ECs over a period of seven days. We intended to identify if HPMECs would have the same network formation as our previously published data, which used Human Umbilical Vein Endothelial Cells (HUVECs) and retinal EC on ASCs, on TCP [27, 28, 29]. Vascular-like networks were observed on TCP after 53 h of co-culture (Supplementary information Figure 3 and Supplementary information video 10).

Supplementary content related to this article has been published online at https://doi.org/10.1016/j.heliyon.2020.e04329.

On PDMS, ASCs readily adhered and during a 72 h proliferation period had formed a confluent monolayer (not shown) onto which ECs were seeded and allowed to form networks for seven days. Within hours, the seeded ECs had adhered and had started to form clusters from which networks emerged (Figure 7a, Supplementary information video 11). The network architecture was virtually completed at approximately 41 h post-seeding of ECs. Thereafter, networks grew and further developed.

Supplementary content related to this article has been published online at https://doi.org/10.1016/j.heliyon.2020.e04329.

The mixed directional topography showed ASC alignment on the directional topography (Figure 7b, Supplementary information video 12) while random orientations were observed on the flat part (Supplementary information Figure 4). This was similar to our earlier findings [25]. Additionally, at 41 h post-seeding of the ECs, they had formed limited networks on the ASCs monolayer of the flat areas but not on the ASCs on the topography. Thus, the networks formation on the topography was reduced compared to the flat controls.

Supplementary content related to this article has been published online at https://doi.org/10.1016/j.heliyon.2020.e04329.

On microsized directional topography, seeded ECs did not form networks on ASCs but instead aligned to the directionality of the aligned ASCs. However, at 41 h post-seeding, limited vascular-like networks formation was observed as ECs with stalk cell and tip cell morphology had appeared (Figure 7c, Supplementary information video 13). This vascular-like network formation became more apparent after nearly 78 h of co-culture (Figure 7c, Supplementary information video 13).

Supplementary content related to this article has been published online at https://doi.org/10.1016/j.heliyon.2020.e04329.

In contrast to ECs seeded directly on gelatin or fibronectin coated PDMS substrates, ECs did not aggregate after seeding on ASC monolayers. Aggregation on PDMS appeared to be EC-specific because ASCs cultured on flat PDMS did not aggregate and instead formed stable monolayers (Supplementary video 14).

Supplementary content related to this article has been published online at https://doi.org/10.1016/j.heliyon.2020.e04329.

ASCs promoted EC networks formation on all substrates. However, the most striking differences were among topography and flat culture substrates (stiff TCP versus softer PDMS) by controlling the vascular-like network formation and the network formation time, respectively. Flat substrates (TCP and PDMS) had larger assemblies of EC networks whereas the substrates with directional topography had smaller aligned vascular-like networks of ECs. The difference between the flat PDMS and the TCP is that PDMS reduced the EC vascular-like network formation time.

3. Discussion

Many tissue engineering approaches rely on anisotropic/directional topography in order to stimulate cells and provide guidance. However, vascularization is of utmost importance in such tissues and topography could seriously affect such vascularization processes [9, 12, 30]. In this study, a directional topographical gradient was used to determine the changes in phenotype of human pulmonary microvascular cells. The importance of addressing topography in a broad sense spanning many different sizes is important as topography remains a powerful approach to generate morphologically distinct tissues with intrinsic anisotropic structure. Vascularization remains a challenge, particularly using coculture systems and the morphological properties as well as cell behavior such as migration and wound healing have been addressed using anisotropic topography [10, 11, 31]. Topography may direct the tissue cell positively but may have a strong impact on the supporting cells that are required to provide more function to the engineered tissues. In our investigation towards EC behavior with respect to a broad range of topography, we found that cells formed vascular-like networks on the PDMS nano/microsized directional topography (positions 0–7 mm) and flat surfaces but was not stable over time and formed aggregates. ECs aligned and remained attached to the surface of the larger microsized directional topography (positions 8–10 mm). ECs seemed to continue proliferating on the surfaces with directional topography gradients since the vascular-like networks reappeared in the same area over time. Mixed topographies showed that aggregates are made of alive cells that once in contact with the directional topography can break into single cells. ASCs provided an appropriate instructive coating for stabilizing EC network formation, even on top of the directional topography that does not support network formation without ASCs, not even when coatings are applied. Upon applying the ASC instructive layer, ECs will not be directly in contact with the aligned topography underneath the ASCs. However, the ASCs are also highly aligned and thereby are likely to at least transmit the directionality stimulus albeit with a different specific topography. Topography-mediated behavior in more complex cell systems making use of multiple layers should also consider such alignments. It was recently shown that aligned fibroblasts deposit their ECM also in an aligned

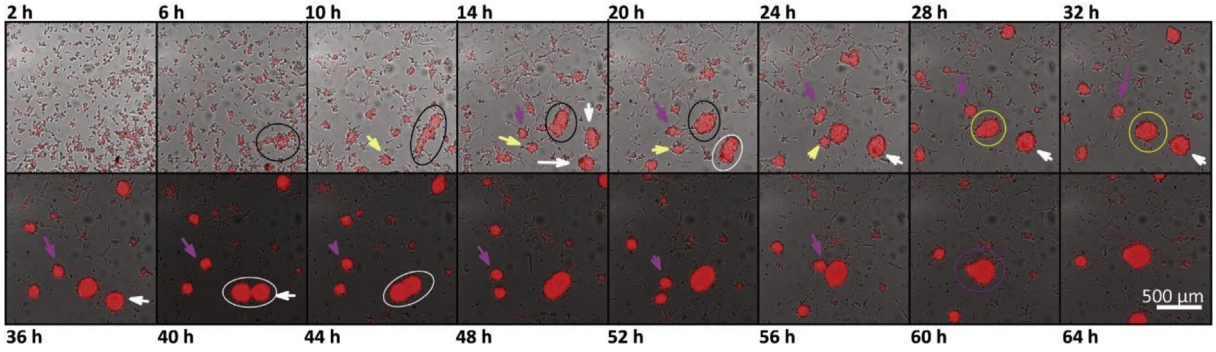

Figure 5. Merge of EC aggregates on a flat PDMS substrate after 64 h of cell culture. Black ellipse shows an aggregate forming after 6 h of cell culture. This aggregate surrounded by the black ellipse merges with other aggregates over time. After 10 h a yellow arrow is pointing at the aggregate that will merge with the previously mentioned aggregate. After 14 h two white arrows depict two aggregates that merge in the next micrograph (20 h) and that will merge after 40 h with the previously mentioned set of aggregates. Finally, the aggregate depicted with a purple arrow merges to the initial aggregate after 56 h of cell culture. Scale bar represents 500 µm.

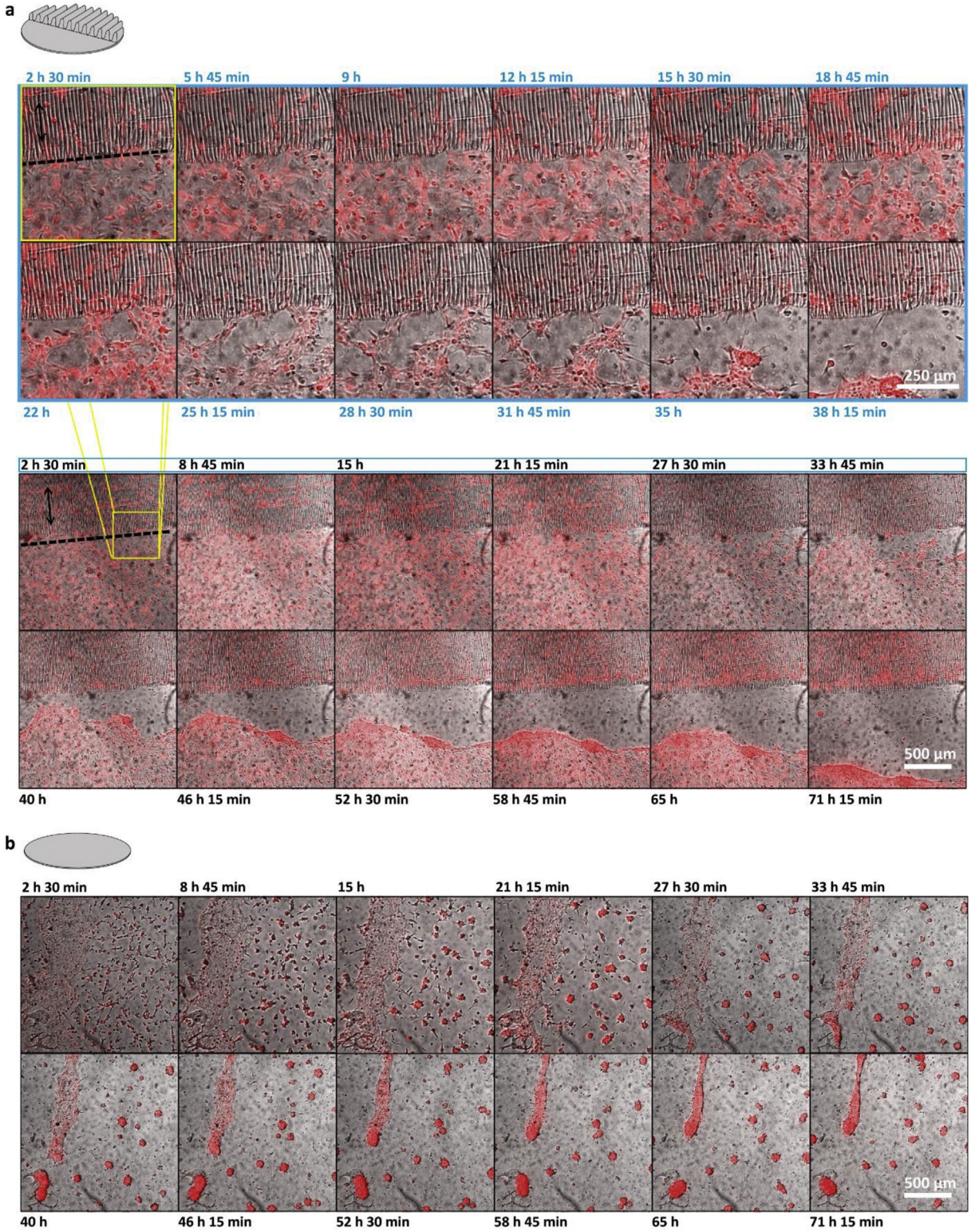

Figure 6. Fibronectin coating reduced the likelihood of vascular-like network formation. **a.** Mixed topography: directional topography running perpendicular to the flat coated with 20 µg per ml fibronectin. Arrow shows the directionality of the topography. Dotted lines show the interface between flat and topography. Upper part is a zoomed-in image of the bottom part and a zoom-in to the first 38 h 15 min of cell culturing. **b.** Flat substrate coated with 20 µg per ml fibronectin. Scale bars are 500 µm.

fashion [32], which would also enable the transmittance of directionality inflicted by the sub-phase.

Gradient systems of thickness have also been investigated. Changing the thickness of Matrigel on a glass coverslip influenced the vascular-like network formation behavior, where the least thick gel formed an EC monolayer and as the gel thickness increased, the vascular-like network formation behavior of HUVECs was observed [33]. Stiffness has been an established factor influencing vascular-like network formation, and we

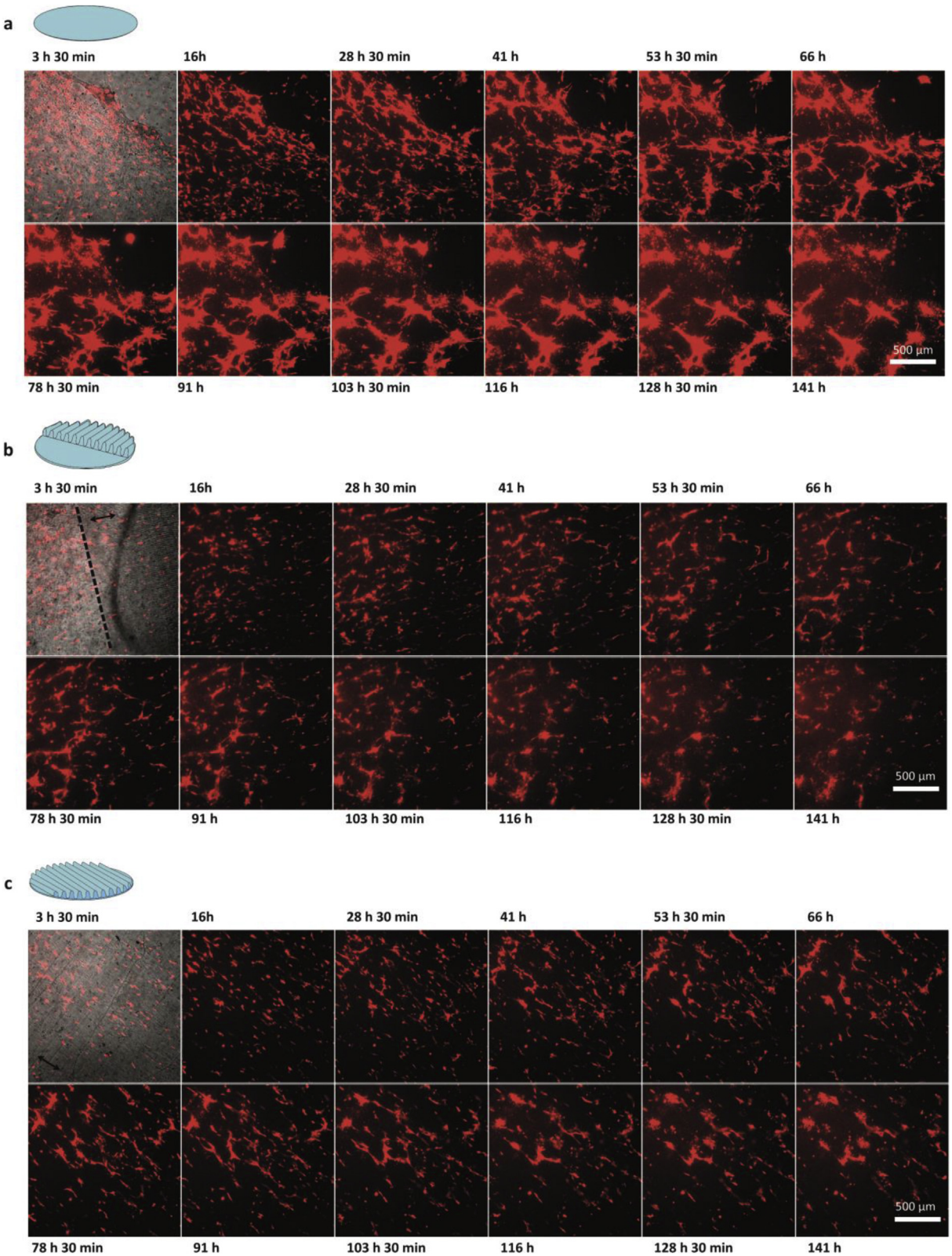

Figure 7. ECs on top of a confluent ASC monolayer. First micrograph in the panels shows a bright field image and subsequent panels show only the ECs dTomato+. Arrows represent the directionality of the topography when applicable. **a.** flat PDMS **b**. mixed directional topography. **c.** Uniform directional topography. Scale bars are 500 µm.

showed that topography also influences the vascular-like network formation properties of ECs. The flat and nanosized topography provided an environment appropriate for networks formation but this was only stabilized by including an ASC instructive coating. This coating, which was softer than the PDMS and provided ECM components, might have allowed the ECs to reorganize their extracellular matrix. In the absence of an ASC coating, the nano and flat surfaces provided an environment appropriate enough for cells to form preliminary networks but favored the cell aggregation process. The larger microsized topography had boundaries that allowed cell alignment and proliferation, but it might have inhibited the cell extracellular matrix reorganization, which discouraged network formation. Therefore, nanosized directional topography and flat surfaces enhanced vascular-like networks and micron-size directional topography encouraged alignment and proliferation of ECs.

Our directional topographical gradient showed how microsized and flat/nanosized topographies affect the cellular phenotype by creating alignment and by producing unstable vascular-like networks, respectively. Previously, nanoscale patterning influencing alignment and proliferation of primary human dermal microvascular ECs has been studied. However, this study used aligned collagen I fibrils with diameters of 30–50 nm [13]. Nakayama *et. al* indicated that ECs aligned along the direction of the nanofibrils without applying a shear-flow. They then applied disturbed shear orthogonal flow (0–259.8 mm per s) and evaluated the cell alignment for 24 h after exposure. They found that the ECs continued to be aligned and that nanopatterning inhibits inflammatory response. Differences in material, feature sizes, and type of ECs could bring distinct responses. Our directional topography could enlighten the different nano and micro-environments that affect the EC alignment, proliferation, and vascular-like network formation capacities for various endothelial cell types. Finding the topography size that aligns the cells in the same way as they aligned as a product of the blood flow and shear stress that the cells are exposed [3] could bring new insights for vascularization in tissue engineering.

A system that combined topographies, albeit non-gradient, had similar dimensions to our directional topography gradient with PDMS patterned surfaces. This system had: aligned gratings of 2 μm ridge, width, and depth; and within the groove nanopatterns of 250 nm parallel and perpendicular to the directionality of the grating [34]. They showed that healthy and diseased (diabetic) human coronary artery endothelial cells responded differently to the PDMS substrates studied. We only evaluated one type of endothelial cell in our gradient system, but previously we have also used the same gradient to identify the behavior of myoblasts [26] and a similar gradient to identify the behavior of ASCs [25] finding that indeed various cell types result in different alignment and differentiation patterns. Future research should include other types of endothelial cells on our topographical gradient to study if the network formation is reproducible among endothelial cells and characterize what are the specific features for each cell type and their relationship between healthy and diseased patients.

Polyurethane nanotopographies and flat surfaces have also been shown to decrease the proliferation of HUVECs and human aortic cells (HAEC) [20]. The influence of various topographies on HUVECs was also recently confirmed using a MultiARChitecture (MARC) chamber showing that topography influences the adhesion and proliferation behavior significantly [35]. However, network formation was not investigated, which is crucial for tissue engineering approaches. We observed that nanosized topography had a similar behavior to the flat where the proliferation of ECs was decreased. However, these topographies, flat and nanosized topography, produced unstable vascular-like networks. This EC response reported here is triggered only by topography; the surface chemistry and stiffness are equal for both surfaces. Difference in topography within the same substrate triggers the cells to form early networks or align. What is more, ECs continued proliferating on the microsized topography which initially populated the nanosized topography and showed rounds of spontaneous network formation connected to the cell confluency. Therefore, we created a combined system in order to try to stabilize the vascular-like network formation behavior by combining the flat topography with the topography that aligned and proliferated the cells.

In this mixed topography we saw aggregate formation on the flat area, and migration and disintegration of these aggregates on the microsized directional topography. Again, this proved that the directional topography induced cell proliferation while the flat surface generated unstable networks that collapsed and aggregated. Additionally, cell confluency played an important role in the disintegration of aggregates. Once the aggregates reached an area of cell confluency, they started to disintegrate in single cells. Migration is important for reendothelialization [36]. Our system showed that different topographies affect the migration ability of the cells. However, the question remains as to whether the directional topography attracted the aggregates or not. Further understanding is needed of the mechanisms involved to identify if the aggregates specifically migrate to the directional topography and why these destabilize on the topography and become single cells again.

Our surfaces had a total exposure time to the plasma treatment of 15 min (15 min for the wrinkled part and 5 min to the flat part). Our plasma treatment might have exposed silanol compounds, which created Reactive Oxygen Species (ROS) once in contact with the cells. In the correct concentration ROS can regulate cell function [37]. High ROS content on PDMS surfaces has been linked with cellular aggregate formation of endothelial cells [38]. Choi *et al.* reported that the cells readily detached from UV/O (UV-induced ozone formation) PDMS surfaces treated for up to 90 min coated with fibronectin, same coating as in our case. They proposed that the fibronectin coating on the UV/O treated surface underwent degradation due to the ROS initial radicals on the surface [38]. Therefore, our treatment had been just enough to trigger the vascular-like networks formation of the cells and allowed the topography to direct the alignment of ECs on the microsized topography. Additionally, the use of an ASC instructive coating was enough to stabilize ECs within the system. It must be noted that the time used here for the plasma treatment is much shorter than reported previously for the UV/O treatments and the difference in surface stiffness was not considered in the former experiments. Thus, from previous studies, plasma treatment beyond 10 min will not substantially affect the stiffness [39, 40]. Besides, the plasma treatment is short-lived and deactivation of the surface (hydrophobic recovery) occurs rapidly, rendering it much less reactive. Nonetheless, such subtle differences between materials chemistry and endothelial cells need to be carefully considered.

4. Conclusion

Endothelial cells respond to topography by altering their phenotype and contact guidance. Microsized topography (wavelengths ranging from 4.8 μm to 9.9 μm and amplitudes ranging from 1015 nm to 2169 nm) caused cell alignment and smaller features and flat PDMS surfaces caused unstable vascular-like networks that formed aggregates able to migrate and disintegrate into single cells upon contact with the larger directional topography. An ASC instructive coating allowed stabilization of the EC vascular-like networks, but even so, the microsized directional topography showed inhibition of network formation compared to its flat counterpart. The study shows that interfacing materials and cells in an artificial fashion, as is often done in the field of tissue engineering, will bring forth unexpected and interesting behaviors. These kinds of behaviors might provide insights into different pathologies, disease models, but also underlying variations in molecular biological mechanisms.

Declarations

Author contribution statement

A. Suarez: Conceived and designed the experiments; Performed the experiments; Analyzed and interpreted the data; Wrote the paper.

P. van Rijn and M. Harmsen: Conceived and designed the experiments; Analyzed and interpreted the data; Contributed reagents, materials, analysis tools or data; Wrote the paper.

I. van der Ham and M. Brinker: Performed the experiments; Analyzed and interpreted the data; Wrote the paper.

Funding statement

This work was supported by Stichting De Cock-Hadders (project number 2019-03) and Nederlandse Organisatie voor Wetenschappelijk Onderzoek (40-00506-98-9021).

Competing interest statement

The authors declare the following conflict of interests: P. van Rijn also is co-founder, scientific advisor, and shareholder of BiomACS BV, a biomedical-oriented screening company.

Additional information

Supplementary content related to this article has been published online at https://doi.org/10.1016/j.heliyon.2020.e04329.

Acknowledgements

We would like to thank the UMCG Microscopy and Imaging Center (UMIC) for their assistance with the microscopy.

STAR*METHODS

Materials and methods

PDMS surfaces

Polydimethylsiloxane (PDMS) directional topography gradients and uniform topography were made as described in our previous work [23, 26]. Briefly, elastomer (Sylgard-184A) and a curing agent (Sylgard 184B) from the kit Dow Corning were mixed by hand, at a mixing ratio of 10:1 w/w, for five minutes. Then, 18 g of mixture was poured into a 12 × 12 cm petri dish and left overnight at room temperature to degas the solution. Then, the PDMS cured for three hours at 70 °C. Next, 9 × 9 cm films were cut and placed in a custom-made stretching device and stretched to 130% of their initial length. PDMS strips of 0.5 × 9 cm, were placed 2 cm apart on the PDMS film in order to create surfaces with mixed topography (flat and wrinkled). For creating different topography directions with respect to the flat area, the PDMS strips were placed perpendicularly or parallel with respect to the stretching direction. For creating gradients, films made were 2 × 2.5 cm, and a metal triangular-shape mask of 1.3 cm long and 1.0 cm wide and a 30° aperture was used to cover the PDMS surface while stretched in a smaller version of the homemade stretching machine. The system, which includes both the stretching machine and PDMS film, was placed in the plasma oven (Diener electronic, model Atto, Ebhausen, Germany). Plasma oxidation was done at 10 mTorr for 600 s at maximum power. Afterwards, tension was slowly released, and directional topography was formed. Post-treatment of the surfaces to guarantee homogeneous stiffness and surface chemistry was performed using plasma treatment at 130 mTorr for 300 s at maximum power. Surfaces were activated for 45 s at 200 mTorr before cell culture.

Sterilization of surfaces. The PDMS was cut (1.5 cm diameter) in the shape and dimension of the culture plate. Then, the circular PDMS pieces containing either the 1 × 1 cm gradients or the mixed topography were washed twice with PBS, sterilized with 70 % ethanol for 10 min, washed again twice with PBS, and finally rinsed with sterile water.

Coating of the surfaces. Endothelial cells need an appropriate protein coating in order to adhere to the PDMS. Therefore, after sterilization of the different PDMS surfaces, coatings were applied using solutions containing 1 μg per ml of gelatin, 1 μg per ml, 10 μg per ml, or 20 μg per ml of human fibronectin in which the samples were left for 20 min at room temperature and then aspirated before cell culture.

AFM characterization

Catalyst NanoScope IV instrument (Bruker, Billerica, MA, USA) and analysis software NanoScope Analysis (Bruker Billerica, MA, USA) were used to measure the directional topography by contact-mode. Cantilever "D" (resonant frequency 18 kHz and spring constant 0.006 N/m) from DNP-10 Bruker's robust Silicon Nitride AFM probe was used for the measurements.

Directional topographical gradient features. The 1 × 1 cm directional topography gradient used for the experiments was characterized previously by AFM [26]. Measurements were taken every 1 mm between 0 and 10 mm across the topography gradient. Below are the results summarized in Table 1.

Table 1. Directional topography gradient features.

Position (mm)	0	1	2	3	4	5	6	7	8	9	10
Wavelength (μm)	1,324	1,520	1,780	2,043	2,320	2,680	3,219	3,889	4,820	6,373	9,935
Amplitude (μm)	0,132	0,176	0,243	0,325	0,391	0,488	0,621	0,780	1,015	1,324	2,169

Cell culture

Human-pulmonary-microvascular-endothelial-cells (HPMECs). Human pulmonary microvascular endothelial cells clone HPMEC-ST1.6R (referred to as HPMEC) were a kind gift of Dr. R.E. Unger, Johannes-Gutenberg University, Mainz, Germany. ECs were lentiviral tagged with EGFP and dTomato as previously described [41]. Culture medium consisting of Roswell Park Memorial Institute (RPMI) 1640 basal medium (Lonza, Basel, Switzerland), supplemented with 1% L-Glutamine (Lonza, Basel, Switzerland), 20% fetal bovine serum (FBS, Life Technologies Gibco/Merck KGaA, Darmstadt, Germany), 1% penicillin/streptomycin (Invitrogen, Thermo Fisher, USA), 50 μg/ml of homemade endothelial cell growth factor (ECGF), and 1%

heparin was used for culturing the HPMECs. Cells were passaged at a 1:3 ratio after detachment with TEP, consisting of 0.1% Trypsin (Fisher Scientific, Ontario, Canada) and 2 mM EDTA (Sigma-Aldrich/Merck KGaA, Darmstadt, Germany). The tissue culture plate was coated with 1 μg per ml gelatin before seeding. ECs were seeded at a density of 3×10^4 cells per cm^2.

Adipose Stem Cells. Adipose stem cells were previously isolated [42]. Culture medium used was high glucose Dulbecco's Modified Eagle's Medium (DMEM; Lonza, Basel, Switzerland), 10% fetal bovine serum (FBS, Life Technologies Gibco/Merck KGaA, Darmstadt, Germany), and 1% penicillin/streptomycin (Invitrogen, Thermo Fisher, USA). Cells were passaged at a 1:3 ratio after detachment with TEP (0.1% Trypsin (Fisher Scientific, Ontario, Canada) and 2 mM EDTA (Sigma-Aldrich/Merck KGaA, Darmstadt, Germany).

Cells were examined using an inverted microscope Invitrogen EVOS FL Cell Imaging System (Life technologies, 5791 Van Allen Way Carlsbad, CA 92008 USA) and an inverted contrasting microscope for living cell applications Leica DM IL (Leica Microsystems GmbH, Germany).

Live imaging with wide field fluorescence microscope Solamere

Endothelial cells were monitored over a period of three days on TCP (Tissue Culture Polystyrene), flat PDMS, and mixed topography (micron-size topography running both parallel and perpendicular to the flat on the same PDMS samples). ECs were seeded at a density of 3×10^4 cells per cm^2. For the experiments involving the mixed topographies, images were recorded every hour at three different spots per sample over three days. This was replicated three times. For the coating experiment, images were recorded every 15 min in two separate spots per sample. Finally, for the co-culture experiment of pre-culture ASCs plus ECs, images were taken every hour for seven days. For all the experiments, bright-field transmitted light and incident light fluorescence were used with a magnification of 5x and camera 1x. Each image corresponded to a surface area of 1670 μm × 1673 μm. Selected areas were monitored over time as it was intended to focus on the interface between flat and structured surfaces.

The microscope used was a Solamere Nipkow Confocal Live Cell Imaging system based on a Leica DM IRE2 inverted microscope with fully motorized objective nosepiece and fluorescence filter cube change, an Andor iXon DV885 EM CCD camera and an intuitive ANDOR IQ software.

Statistical analysis

A Shapiro-Wilk normality test was applied to the Solamere videos after 10, 20 and 40 h in flat, and mixed topographies. Following that, a One-way-ANOVA and Tukey's multiple comparison test was conducted to evaluate the material influence in the aggregate morphology. GraphPad Prism 7.04 (GraphPad Software, Inc. San Diego, US) was used for the statistics analysis.

References

[1] J. Rouwkema, A. Khademhosseini, Vascularization and angiogenesis in tissue engineering: beyond creating static networks, Trends Biotechnol. 34 (2016) 733–745.

[2] A.M. Greiner, A. Sales, H. Chen, S.A. Biela, D. Kaufmann, R. Kemkemer, Nano-and microstructured materials for in vitro studies of the physiology of vascular cells, Beilstein J. Nanotechnol. 7 (2016) 1620–1641.

[3] D.E.J. Anderson, M.T. Hinds, Endothelial cell micropatterning: methods, effects, and applications, Ann. Biomed. Eng. 39 (2011) 2329.

[4] E.E. Van Haaften, C.V.C. Bouten, N.A. Kurniawan, Vascular mechanobiology: towards control of in situ regeneration, Cells 6 (2017) 19.

[5] L. Lamalice, F. Le Boeuf, J. Huot, Endothelial cell migration during angiogenesis, Circ. Res. 100 (2007) 782–794.

[6] D. Hielscher, C. Kaebisch, B.J.V. Braun, K. Gray, E. Tobiasch, Stem cell sources and graft material for vascular tissue engineering, Stem Cell Rev. Rep. 14 (2018) 642–667.

[7] J. Park, D.-H. Kim, H.-N. Kim, C.J. Wang, M.K. Kwak, E. Hur, K.-Y. Suh, S.S. An, A. Levchenko, Directed migration of cancer cells guided by the graded texture of the underlying matrix, Nat. Mater. 15 (2016) 792.

[8] J. Park, D.-H. Kim, A. Levchenko, Topotaxis: a new mechanism of directed cell migration in topographic ECM gradients, Biophys. J. 114 (2018) 1257–1263.

[9] G. Stefopoulos, F. Robotti, V. Falk, D. Poulikakos, A. Ferrari, Endothelialization of rationally microtextured surfaces with minimal cell seeding under flow, Small 12 (2016) 4113–4126.

[10] D. Franco, F. Milde, M. Klingauf, F. Orsenigo, E. Dejana, D. Poulikakos, M. Cecchini, P. Koumoutsakos, A. Ferrari, V. Kurtcuoglu, Accelerated endothelial wound healing on microstructured substrates under flow, Biomaterials 34 (2013) 1488–1497.

[11] P. Uttayarat, M. Chen, M. Li, F.D. Allen, R.J. Composto, P.I. Lelkes, Microtopography and flow modulate the direction of endothelial cell migration, Am. J. Physiol. Hear. Circ. Physiol. 294 (2008) 1027–1035.

[12] J.T. Morgan, J.A. Wood, N.M. Shah, M.L. Hughbanks, P. Russell, A.I. Barakat, C.J. Murphy, Integration of basal topographic cues and apical shear stress in vascular endothelial cells, Biomaterials 33 (2012) 4126–4135.

[13] K.H. Nakayama, V.N. Surya, M. Gole, T.W. Walker, W. Yang, E.S. Lai, M.A. Ostrowski, G.G. Fuller, A.R. Dunn, N.F. Huang, Nanoscale patterning of extracellular matrix alters endothelial function under shear stress, Nano Lett. 16 (2015) 410–419.

[14] L.E. Dickinson, M.E. Moura, S. Gerecht, Guiding endothelial progenitor cell tube formation using patterned fibronectin surfaces, Soft Matter. 6 (2010) 5109–5119.

[15] J. Lafaurie-Janvore, E.E. Antoine, S.J. Perkins, A. Babataheri, A.I. Barakat, A simple microfluidic device to study cell-scale endothelial mechanotransduction, Biomed. Microdevices 18 (2016) 63.

[16] M.W. Hagen, M.T. Hinds, Static spatial growth restriction micropatterning of endothelial colony forming cells influences their morphology and gene expression, PloS One 14 (2019), e0218197.

[17] T. Govindarajan, R. Shandas, Microgrooves encourage endothelial cell adhesion and organization on shape-memory polymer surfaces, ACS Appl. Bio Mater. 2 (2019) 1897–1906.

[18] Y.-K. Hsieh, K.-P. Hsu, S.-K. Hsiao, K.A.V. Gorday, T. Wang, J. Wang, Laser-pattern induced contact guidance in biodegradable microfluidic channels for vasculature regeneration, J. Mater. Chem. B. 6 (2018) 3684–3691.

[19] P. Uttayarat, A. Perets, M. Li, P. Pimton, S.J. Stachelek, I. Alferiev, R.J. Composto, R.J. Levy, P.I. Lelkes, Micropatterning of three-dimensional electrospun polyurethane vascular grafts, Acta Biomater. 6 (2010) 4229–4237.

[20] S.J. Liliensiek, J.A. Wood, J. Yong, R. Auerbach, P.F. Nealey, C.J. Murphy, Modulation of human vascular endothelial cell behaviors by nanotopographic cues, Biomaterials 31 (2010) 5418–5426.

[21] A. Sales, A.W. Holle, R. Kemkemer, Initial contact guidance during cell spreading is contractility-independent, Soft Matter. 13 (2017) 5158–5167.

[22] J. Hu, C. Hardy, C.M. Chen, S. Yang, A.S. Voloshin, Y. Liu, Enhanced cell adhesion and alignment on micro-wavy patterned surfaces, PloS One 9 (2014), e104502.

[23] Q. Zhou, P.T. Kuhn, T. Huisman, E. Nieboer, C. van Zwol, T.G. van Kooten, P. van Rijn, Directional nanotopographic gradients: a high-throughput screening platform for cell contact guidance, Sci. Rep. 5 (2015) 16240.

[24] Q. Zhou, O. Castañeda Ocampo, C.F. Guimarães, P.T. Kühn, T.G. Van Kooten, P. Van Rijn, Screening platform for cell contact guidance based on inorganic biomaterial micro/nanotopographical gradients, ACS Appl. Mater. Interfaces 9 (2017) 31433–31445.

[25] G.R. Liguori, Q. Zhou, T.T.A. Liguori, G.G. Barros, P.T. Kühn, L.F.P. Moreira, P. van Rijn, M.C. Harmsen, Directional topography influences adipose mesenchymal stromal cell plasticity: prospects for tissue engineering and fibrosis, Stem Cells Int. (2019) 5387850.

[26] A.M. Almonacid Suarez, Q. Zhou, P. van Rijn, M.C. Harmsen, Directional topography gradients drive optimum alignment and differentiation of human myoblasts, J. Tissue Eng. Regen. Med. 13 (2019) 2234–2245.

[27] G. Hajmousa, E. Przybyt, F. Pfister, G.A. Paredes-Juarez, K. Moganti, S. Busch, J. Kuipers, I. Klaassen, M.J.A. van Luyn, G. Krenning, Human adipose tissue-derived stromal cells act as functional pericytes in mice and suppress high-glucose-induced proinflammatory activation of bovine retinal endothelial cells, Diabetologia 61 (2018) 2371–2385.

[28] G. Hajmousa, A.A. Elorza, V.J.M. Nies, E.L. Jensen, R.A. Nagy, M.C. Harmsen, Hyperglycemia induces bioenergetic changes in adipose-derived stromal cells while their pericytic function is retained, Stem Cells Dev. 25 (2016) 1444–1453.

[29] V. Terlizzi, M. Kolibabka, J.K. Burgess, H.P. Hammes, M.C. Harmsen, The pericytic phenotype of adipose tissue-derived stromal cells is promoted by NOTCH2, Stem Cell. 36 (2018) 240–251.

[30] Y. Lei, O.F. Zouani, M. Rémy, C. Ayela, M.C. Durrieu, Geometrical microfeature cues for directing tubulogenesis of endothelial cells, PloS One 7 (2012), 0041163.

[31] S. Li, S. Bhatia, Y.L. Hu, Y.T. Shiu, Y.S. Li, S. Usami, S. Chien, Effects of morphological patterning on endothelial cell migration, Biorheology 38 (2001) 101–108.

[32] L. Yang, L. Ge, P. van Rijn, Synergistic effect of cell-derived extracellular matrices and topography on osteogenesis of mesenchymal stem cells, ACS Appl. Mater. Interfaces 12 (2020) 25591–25603.

[33] C.D. Davidson, W.Y. Wang, I. Zaimi, D.K.P. Jayco, B.M. Baker, Cell force-mediated matrix reorganization underlies multicellular network assembly, Sci. Rep. 9 (2019) 12.

[34] M.F.A. Cutiongco, B.M.X. Chua, D.J.H. Neo, M. Rizwan, E.K.F. Yim, Functional differences between healthy and diabetic endothelial cells on topographical cues, Biomaterials 153 (2018) 70–84.
[35] M. Kukumberg, Y. Yao, S.H. Goh, D.J.H. Neo, J.Y. Yao, E.K.F. Yim, Evaluation of the topographical influence on the cellular behavior of human umbilical Vein endothelial cells, Adv. Biosyst. 2 (2018) 1–17.
[36] S. Li, N.F. Huang, S. Hsu, Mechanotransduction in endothelial cell migration, J. Cell. Biochem. 96 (2005) 1110–1126.
[37] M. Yasuda, Y. Ohzeki, S. Shimizu, S. Naito, A. Ohtsuru, T. Yamamoto, Y. Kuroiwa, Stimulation of in vitro angiogenesis by hydrogen peroxide and the relation with ETS-1 in endothelial cells, Life Sci. 64 (1998) 249–258.
[38] J.S. Choi, T.S. Seo, Facile endothelial cell micropatterning induced by reactive oxygen species on polydimethylsiloxane substrates, Biomaterials 84 (2016) 315–322.
[39] P.T. Kuhn, Q. Zhou, T.A.B. van der Boon, A.M. Schaap-Oziemlak, T.G. van Kooten, P. van Rijn, Double linear gradient biointerfaces for determining two- parameter dependent stem cell behavior, ChemNanoMat 2 (2016) 407.
[40] Q. Zhou, L. Ge, C.F. Guimarães, P.T. Kühn, L. Yang, P. van Rijn, Development of A Novel orthogonal double gradient for high-throughput screening of mesenchymal stem cells, Adv. Mater. Interfaces. 5 (2018) 1800504.
[41] A.M. Almonacid Suarez, M.G.L. Brinker, L.A. Brouwer, I. van der Ham, P. van Rijn, M.C. Harmsen, The influences of directional topography in myotube and endothelial alignment, differentiation, and extracellular matrix organization for tissue engineering of skeletal muscle 13 (2020) 2234–2245.
[42] E. Przybyt, G. Krenning, M.G.L. Brinker, M.C. Harmsen, Adipose stromal cells primed with hypoxia and inflammation enhance cardiomyocyte proliferation rate in vitro through STAT3 and Erk1/2, J. Transl. Med. 11 (2013) 39.